Flow-Based Grid Coarsening for Transport Simulations

Vera Louise Hauge, Knut–Andreas Lie, and Jostein R. Natvig
Department of Applied Mathematics, SINTEF ICT, Oslo, Norway

Motivation

To optimise the recovery from brown and mature fields, there is a growing need for multi-fidelity modelling. To this end, one needs accurate and robust upgridding methods that can (automatically) coarsen the grid to reduce the number of degrees of freedom to a level that is sufficient to resolve flow physics and satisfy requirements on computational costs, moving seamlessly between different spatial resolutions while preserving the important characteristics of an underlying high-resolution geo-cellular model.

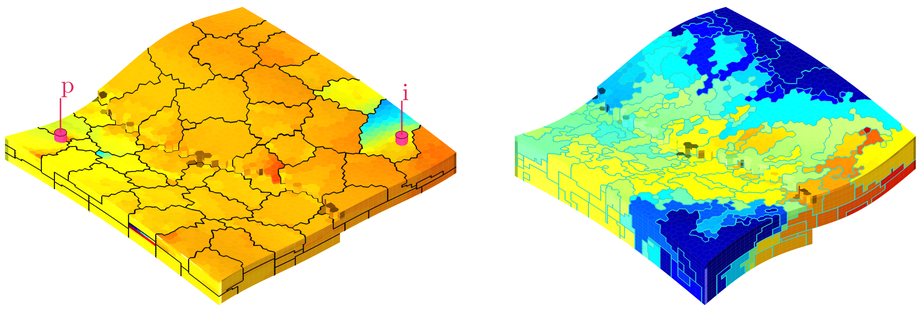

Pressure and transport equations are different in nature and require different strategies for optimal upgridding. In particular, the grid used in transport calculations should be adapted to the flow patterns predicted by the pressure equation to optimize accuracy for a given number of coarse blocks.

Flow-Based Coarsening

Assumptions:

- a matching, unstructured, polyhedral grid with n cells c_i,
- a mapping $\mathcal{N}(c)$ between cell c and its nearest neighbours,
- a set of fluxes v_{ij} at the interface γ_{ij} between cells c_i and c_j.

The grid will typically be a high-resolution geological model, for which fluxes can be computed by a multiscale pressure solver [2].

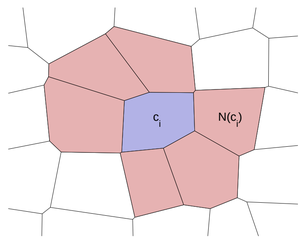

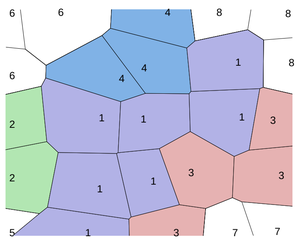

We seek a coarse grid that:

- adapts to the flow pattern predicted by the fluxes v_{ij},
- is formed by grouping sets of cells into N blocks B_ℓ,
- is described by a partition vector p with n elements, for which element p_i assumes the value ℓ if cell c_i is member of block B_ℓ.

Herein, the coarse grid will be generated using an ad-hoc four-step method by Aarnes et al. [1] using the logarithm of the flux, $g(c_i) \propto \log|\vec{v}(c_i)|$, as indicator function:

1. *Compute an initial partitioning*. Segment $g(c_i)$ into ten uniform bins. Each bin $\tilde{B}_\ell$ may consist of a multiply connected set of cells and must be postprocessed and split into singly-connected blocks.

   Illustration: quarter-five spot for a 50×50 excerpt of Layer 68 of SPE 10 [3].

2. *Merge small blocks*. If a block B' has too small volume, $|B'| < \frac{N_L}{n}|\Omega|$, it is merged with the neighbouring block B that has the closest g-value defined as $g(B)|B| = \int_B g(c)\,dx$.
3. Refine blocks with too much flow. If $\int_B g(c)\,dx > \frac{N_U}{n}\int_\Omega g(c)\,dx$, then
   - ▷ Pick an arbitrary cell c_0 belonging to ∂B.
   - ▷ Find the cell $c_1 \subset B$ that is furthest away from c_0 and define $B' = c_1$.
   - ▷ Progressively enlarge B' by adding cells surrounding B'; that is, add $c \subset \mathcal{N}(B')$ if $c \not\subset B'$ until the threshold is exceeded.
   - ▷ Define $B = B \setminus B'$ and continue to refine B if the upper bounds are still violated.
4. *Repeat Step 2*.

This algorithm is a particular example from a large class of (semi-) automated upgridding algorithms based upon agglomeration of cells according to *a priori* or flow-based indicator functions [4].

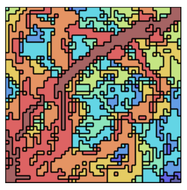
Step 1: 304 blocks

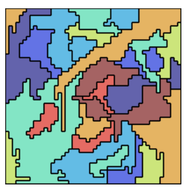
Step 2: 29 blocks

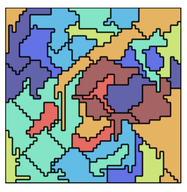
Step 3: 47 blocks

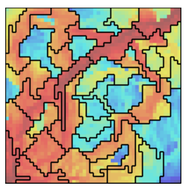
Step 4: 39 blocks

Imposing A Priori Geometrical Shapes

- Original algorithm from [1] works best when flow is strongly dominated by geological heterogeneity. Compared with uniform coarse grids on layers of SPE 10 [3]
  - ▷ much better accuracy on fluvial layers (Upper Ness),
  - ▷ slightly worse accuracy on smooth layers (Tarbert).

  Highly irregular blocks ⇒ more neighbours ⇒ stronger coupling in nonlinear system
- New ideas:
  - ▷ intersect initial segmentation with *a priori* partitions,
  - ▷ use span in $\log|v|$ to set initial bins in Step 1,
  - ▷ improve refinement in Step 3 by extending $\mathcal{N}(c_i)$ or by using e.g., Metis.

Example: Layer 1 from SPE 10, intersection with uniform Cartesian coarse grid.

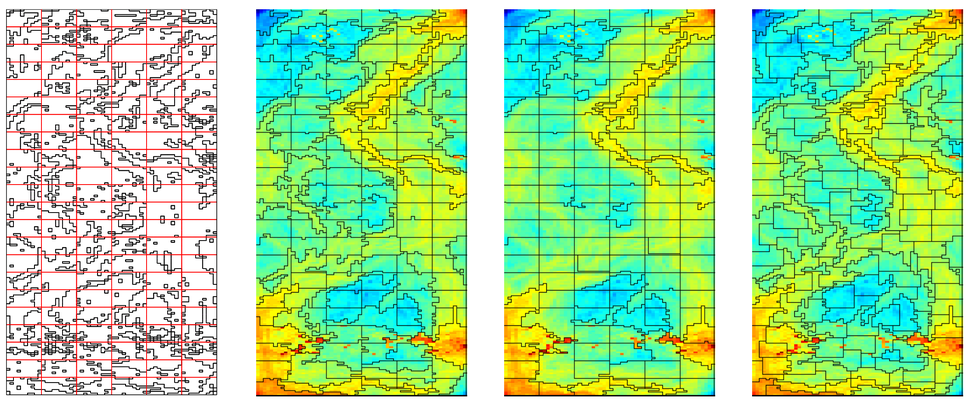

Initial intersection | 10 bins, 178 blocks, 852 faces | $\log|v|$ bins, 154 blocks, 709 faces | Original, 9-neighbour, 188 blocks, 930 faces

Imposing Geological Constraints

The initial partitioning can also be intersected with *a priori* geological information (facies, saturation regions, capillary regions, etc) that need to be preserved during the coarsening.

Example: Restricting blocks to 2D facies distribution.

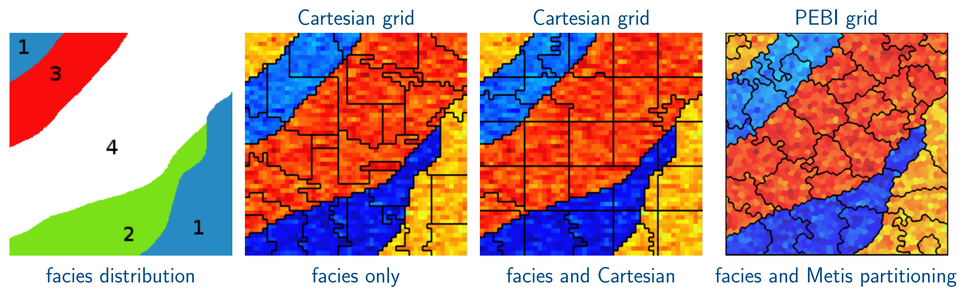

facies distribution | facies only | facies and Cartesian | facies and Metis partitioning

Example: Restriction to saturation regions for a SAIGUP realisation [5].

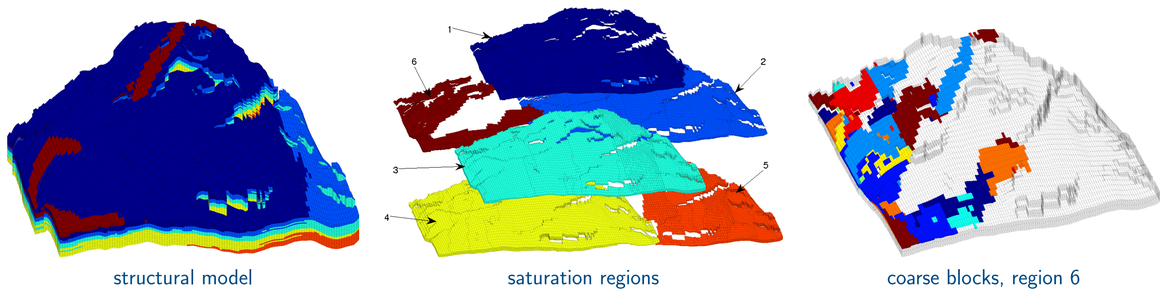

structural model | saturation regions | coarse blocks, region 6

Discretizations and Numerical Errors

Consider incompressible, immiscible, two-phase flow: $\phi\partial_t S + \vec{v}\cdot\nabla f(S) = h_S$. A conservative coarse-grid discretization is obtained by summing a standard single-point upwind discretization for all cells in a block:

$$S_\ell^{n+1} = S_\ell^n + \frac{\Delta t}{\int_{B_\ell}\phi\,dx}\int_{B_\ell} h_S(S^{n+1})\,dx - \frac{\Delta t}{\int_{B_\ell}\phi\,dx}\Big[f(S_\ell^{n+1})\sum_{\gamma_{ij}\subset\partial B_\ell}\max(v_{ij},0) - \sum_{k\neq\ell}\Big(f(S_k^{n+1})\sum_{\gamma_{ij}\subset\Gamma_{k\ell}}\min(v_{ij},0)\Big)\Big]$$

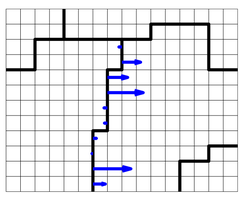

If there is a bi-directional flow across $\Gamma_{k\ell} = \partial B_k \cap \partial B_\ell$, then the phase-flux across $\Gamma_{k\ell}$ is approximated using both S_ℓ and S_k. Alternatively, one can use the net fluxes to define upwind directions, giving a coarse-scale upwind method.

Example: Average errors in saturation and water cut for the two formation in SPE 10 [3].

		Tarbert formation				Upper Ness formation			
		10 bins	$\log\|v\|$ bins	Original	Cartesian	10 bins	$\log\|v\|$ bins	Original	Cartesian
	$E_s(\mathcal{P}\mathcal{R}S_f, S_f)$	0.0920	0.0941	0.1042	0.0911	0.1394	0.1371	0.1355	0.1772
Bi-dir	$E_s(\mathcal{P}S_c, S_f)$	0.2071	0.1910	0.2426	0.1687	0.2180	0.2124	0.2243	0.2305
	$E_s(S_c, \mathcal{R}S_f)$	0.1784	0.1599	0.2100	0.1381	0.1572	0.1522	0.1683	0.1604
	$E_w(w_c, w_f)$	0.0649	0.0695	0.0773	0.0701	0.0613	0.0609	0.0668	0.0982
Upwind	$E_s(\mathcal{P}S_c, S_f)$	0.1591	0.1607	0.1875	0.1619	0.1827	0.1795	0.1862	0.2191
	$E_s(S_c, \mathcal{R}S_f)$	0.1220	0.1237	0.1459	0.1302	0.1155	0.1135	0.1225	0.1486
	$E_w(w_c, w_f)$	0.0349	0.0473	0.0444	0.0647	0.0232	0.0237	0.0325	0.0844
	# blocks: span	232–268	217–261	233–312	264	202–234	205–241	220–303	264
	# blocks: mean	249	236	275	264	216	222	264	264
	# faces: mean	1175	1069	1363	1090	1049	1070	1309	1090

Here, (S_f, w_f) and (S_c, w_c) denote the saturation and water cut computed on fine and coarse grid, $\mathcal{R}$ the restriction from fine to coarse grid, $\mathcal{P}$ the prolongation from coarse to fine grid, and

$$E_s(q,p) = \frac{1}{T}\int_0^T \frac{\|[q(\cdot,t)-p(\cdot,t)]\phi(\cdot)\|_1}{\|p(\cdot,t)\phi(\cdot)\|_1}\,dt, \qquad E_w(w_1,w_2) = \frac{\|w_1(\cdot)-w_2(\cdot)\|_2}{\|w_2(\cdot)\|_2}.$$

Dynamically Adaptive Grids

- Inaccurate representation of strong displacement fronts can lead to significant errors.
- **Idea:** Refine dynamically around strong fronts.
- For a Buckley–Leverett displacement:
  - ▷ Unswept region ahead of the displacement: coarse grid.
  - ▷ Swept region behind the front: coarse grid.
  - ▷ At the front: fine or intermediate grid.

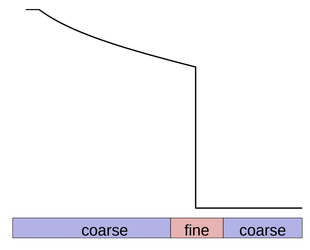

Example: Layer 37 from Model 2 of the SPE 10 benchmark [3].

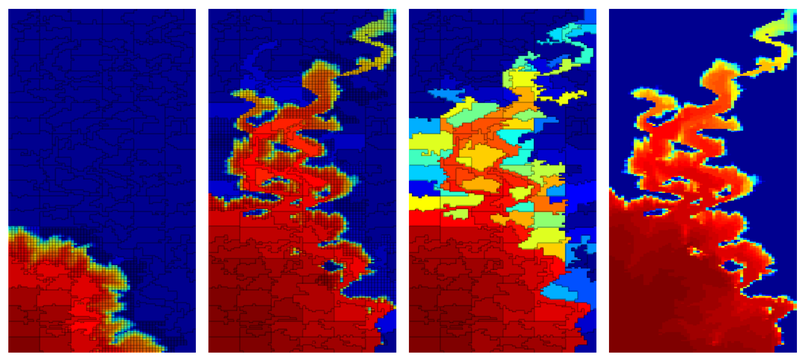

Adaptive, t=0.1 PVI | Adaptive, t=0.5 PVI | Coarse, t=0.5 PVI | Fine grid, t=0.5 PVI

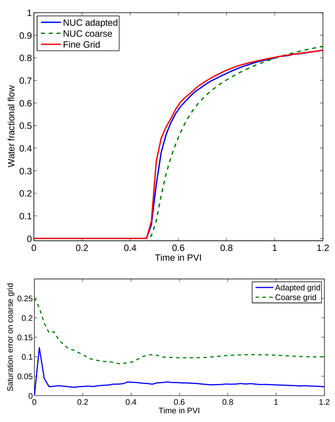

References

[1] J. E. Aarnes, V. L. Hauge, and Y. Efendiev, Y. Coarsening of three-dimensional structured and unstructured grids for subsurface flow. *Adv. Water Resour.*, 30(11):2177–2193, 2007.

[2] J. E. Aarnes, S. Krogstad, and K.-A. Lie. Multiscale mixed/mimetic methods on corner-point grids. *Comput. Geosci.*, 12(3):297–315, 2008. doi:10.1007/s10596-007-9072-8

[3] M. A. Christie and M.J. Blunt. Tenth SPE comparative solution project: A comparison of upscaling techniques. *SPE Reservoir Eval. Eng.*, 4:308–317, 2001. Url: `http://www.spe.org/csp/`.

[4] V. L. Hauge, K.-A. Lie, and J. R. Natvig. Grid coarsening based on agglomeration for multi-fidelity transport solvers. Preprint, 2010. `http://www.sintef.no/Geoscale/`

[5] T. Manzocchi et al. Sensitivity of the impact of geological uncertainty on production from faulted and unfaulted shallow-marine oil reservoirs: objectives and methods. *Petrol. Geosci.*, 14(1):3–15, 2008.

[6] Matlab Reservoir Simulation Toolbox. `http://www.sintef.no/Projectweb/MRST/`